

# Surface Circulation in the Eastern Central North Atlantic

J. H. Bettencourt & C. Guedes Soares

*Centre for Marine Technology and Ocean Engineering (CENTEC), Instituto Superior Técnico, Universidade de Lisboa, Lisbon, Portugal*

**ABSTRACT:** The surface circulation in the Eastern Central North Atlantic is studied using a high resolution primitive equation regional ocean model simulation. The model is forced by climatological surface momentum, heat and freshwater fluxes and open ocean boundary conditions. Comparisons with drifter-derived velocity estimates show that the model is able to reproduce the main features of the surface circulation in the coastal Portuguese waters and in the Portuguese archipelagos of Azores and Madeira. The Azores Current (AzC) appears as a meandering zonal jet centered around 34° N, flowing eastward. The western Iberian margin is characterized by an seasonal upwelling regime where a cooling of near shore waters occurs between late spring and early autumn. Mesoscale activity is present in the upwelling front as coastal filaments and mesoscale eddies. The northward Portugal Coastal Counter Current is a prominent feature of the coastal circulation.

## 1 INTRODUCTION

The Eastern Central North Atlantic (ECNA) is the stretch of the eastern north Atlantic basin between the subtropical and subpolar gyres, possibly including their northern and southern borders, respectively. The region also coincides with the Portuguese territorial waters and its Economic Exclusive Zone, whose monitoring and management is a national maritime policy goal. To aid in this goal, the OBSERVA.FISH project (Piecho-Santos et al., 2020) aims to provide datasets from autonomous ocean observing systems, to be used in, among other purposes, support of an ocean forecast system that will be developed based on the simulations presented herein.

Although most of the large scale circulation patterns in the North Atlantic reside outside of the ECNA (Tomczak and Godfrey, 2013), the ECNA has been a region of intense oceanographic research due to the special characteristics of its features such as the Azores current (AzC), a permanent zonal jet subject to an intense meandering regime set by its baroclinicity (Alves et al., 2002), the Mediterranean Outflow (MO), that carries heat and salt in to the northern basin and partially regulates the weather at those latitudes (Baringer & Price, 1997; Ellett, 1993) or the West Africa and West Iberia upwelling systems (WibUS), that comprise the northernmost section of the North Atlantic Upwelling Region (Relvas et al., 2007). Earlier modeling studies such as Jia (2000), Johnson & Stevens (2000), Peliz et al. (2007) have focused on these aspects of the circulation in the ECNA.

The eastward flowing AzC is part of the northern branch of the Eastern Subtropical Gyre, that also includes the southward Canary Current and the western North Equatorial Current and is a permanent feature of the region's circulation (Gould, 1985; Traon and Mey, 1994). Localized between 33°N-36° N, it crosses the Mid-Atlantic Ridge and flows towards the Gulf of Cadiz. The AzC is a deep (up to 1000 m) current 200 km wide (Stramma and Müller, 1989). Its average transport is 10-12 Sv (1 Sv =  $10^6 \text{ m}^3\text{s}^{-1}$ ) and has a convoluted topology due to its meandering jet character. Average speeds are 0.1-0.15  $\text{ms}^{-1}$  (Klein and Siedler, 1989).

The AzC is associated to a thermohaline front, the Azores Front, that separates the eastern subtropical and subpolar gyres. In the Azores Current and Front system, temperature and salinity jumps of 2°C and 0.3 PSU have been registered. Its convoluted nature has been attributed to quasi-stationary Rossby waves originated in the eastern boundary of the Canary Basin and to baroclinic instabilities of the AzC jet. Meanders form to the north (cyclonic) and to the south (anticyclonic) of the AzC jet core and mesoscale eddies with typical diameter of 200 km have been observed in both flanks of the front (Pingree et al., 1999).

The WibUS is a seasonal upwelling system located in the western coast of the Iberian Peninsula. In the summer, the Azores High strengthens and is displaced northward, setting up upwelling favorable (equatorward) winds over the western Iberian coast that force an offshore Ekman transport and subsequent upwelling of subsurface cold, nutrient rich waters. Due to geostrophic adjustment, an equatorward

jet is formed at the surface compensated by poleward subsurface flows. Coastal upwelling filaments extending to 200 – 250 km offshore and exporting coastal waters are a common feature of the WIBUS and are formed by either topographic forcing or upwelling front instabilities (Haynes et al., 1993).

In this work we employ a the climatological simulation with the aim of reproducing the equilibrium structure of the region's circulation and the mesoscale variability that is essentially determined by the instabilities of large-scale structures such as currents and fronts.

In section 2 the circulation model and the ECNA configuration are described. Section 3 describes the results and section 4 provides the conclusions.

## 2 DATA AND METHODS

The model used in this work is the Regional Ocean Modelling System (ROMS, Shchepetkin & McWilliams 2005, 2003). ROMS is a free-surface terrain-following model which solves the primitive equations using the Boussinesq and hydrostatic approximations. In the primitive equation framework, the prognostic variables are the zonal and meridional velocity components ( $u, v$ ) and the free surface elevation  $\zeta$ . The momentum equations in Cartesian coordinates are (Haidvogel et al., 2008):

$$\frac{\partial(H_z u)}{\partial t} + \frac{(uH_z u)}{\partial x} + \frac{(vH_z u)}{\partial y} + \frac{(\Omega H_z u)}{\partial s} - fH_z v = -\frac{H_z}{\rho_0} \frac{\partial p}{\partial x} - H_z g \frac{\partial \zeta}{\partial x} - \frac{\partial}{\partial s} \left( \overline{u'w'} - \frac{v}{H_z} \frac{\partial u}{\partial s} \right), \quad (1)$$

$$\frac{\partial(H_z v)}{\partial t} + \frac{(uH_z v)}{\partial x} + \frac{(vH_z v)}{\partial y} + \frac{(\Omega H_z v)}{\partial s} + fH_z u = -\frac{H_z}{\rho_0} \frac{\partial p}{\partial y} - H_z g \frac{\partial \zeta}{\partial y} - \frac{\partial}{\partial s} \left( \overline{v'w'} - \frac{v}{H_z} \frac{\partial v}{\partial s} \right), \quad (2)$$

$$0 = -\frac{1}{\rho_0} \frac{\partial p}{\partial s} - \frac{g}{\rho_0} H_z \rho, \quad (3)$$

where (3) is the vertical momentum equation, which in the hydrostatic approximation is a simple relationship between the vertical pressure gradient and the weight of the fluid column. The continuity equation is:

$$\frac{\partial \zeta}{\partial t} + \frac{\partial(H_z u)}{\partial x} + \frac{\partial(H_z v)}{\partial y} + \frac{\partial(H_z \Omega)}{\partial s} = 0, \quad (4)$$

and the scalar transport equation is:

$$\frac{\partial(H_z C)}{\partial t} + \frac{\partial(uH_z C)}{\partial x} + \frac{\partial(vH_z C)}{\partial y} + \frac{\partial(\Omega H_z C)}{\partial s} = -\frac{\partial}{\partial s} \left( \overline{c'w'} - \frac{v}{H_z} \frac{\partial C}{\partial s} \right) + C_{source}. \quad (5)$$

In (1-5)  $s$  is a vertical stretched coordinate that varies from  $s=-1$  (bottom) to  $s=0$  (surface). The vertical grid stretching parameter is  $H_z = \partial z / \partial s$  and  $\Omega$  is the vertical velocity in the  $s$  coordinate. The Coriolis parameter is  $f$ ,  $p$  is the hydrostatic pressure and  $g$  is the acceleration of gravity. An overbar denotes aver-

aged quantities, primed ( $'$ ) variables are departures from the average and  $\nu$  is molecular diffusivity (momentum or scalar). Vertical turbulent momentum and tracer fluxes are:

$$\overline{u'w'} = K_M \frac{\partial u}{\partial z}; \quad \overline{v'w'} = -K_M \frac{\partial v}{\partial z}; \quad \overline{c'w'} = -K_H \frac{\partial p}{\partial z}, \quad (6)$$

where  $K_M$  and  $K_H$  are momentum and tracer eddy diffusivities. The equation of state for seawater is given by  $\rho = f(C, p)$ .  $C_{source}$  is the tracer source/sink term.

ROMS is highly configurable for realistic applications and has been applied to a wide variety of space and time scales across the globe (Haidvogel et al., 2008).

The model domain (Fig. 1) is part of the Eastern Central North Atlantic and covers the western Iberian margin extending to the Azores and Madeira archipelagos (34.4° to 5.7°W and 29° to 46°N). The average horizontal resolution is 4.2 km in the meridional direction and 4.4 km in the zonal direction. The vertical discretization used 20 sigma layers, stretched to increase the resolution near the surface and bottom. The bathymetry is interpolated from ETOPO and smoothed to satisfy a topographic stiffness-ratio of 0.2 (Haidvogel & Beckmann, 1999). The minimum depth used is 10 m.

The model configuration uses a third-order upstream advection scheme for momentum and tracers, a fourth-order centred scheme for vertical advection of momentum and tracers, and the KPP scheme for vertical mixing (Large et al., 1994). Explicit horizontal momentum and tracer diffusion is set to zero. Bottom drag uses a quadratic law with drag coefficient of 0.003.

The model was run in climatological mode where a yearly cycle was repeated for 20 years. The model was forced by surface monthly climatological momentum, heat, freshwater and shortwave radiation fluxes from the Comprehensive Ocean-Atmosphere Data Set (COADS, Woodruff et al (1987)), that collects global weather observations taken near the ocean's surface since 1854, primarily from merchant ships. At the open boundaries, values of 2D (barotropic) and 3D (baroclinic) velocities, and active

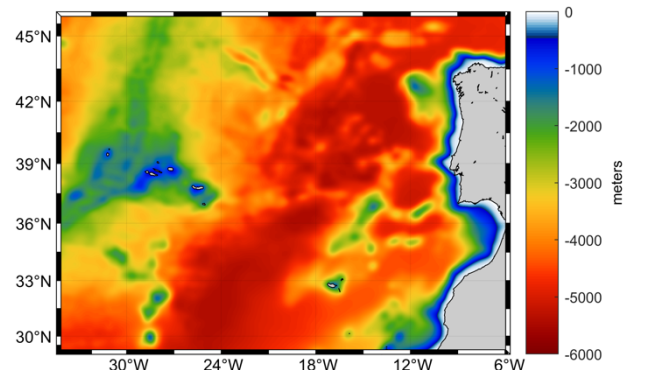


Figure 1. Domain of the ECNA simulation.

tracers (potential temperature and salinity) were nudged to climatological values. The offline nesting procedure employed here used a nudging region of 40 km along the model boundaries. In this layer, the 3-D model variables (temperature, salinity, and currents) were pushed toward their climatological values. The nudging time scale was set to 5 days at the boundaries, decaying linearly to zero inside the nudging layer. At the boundaries, outgoing radiation conditions were used for the baroclinic variables (Marchesiello et al., 2001). Climatological sea surface height and barotropic currents were imposed at the boundaries using Chapman boundary conditions (Chapman, 1985).

### 3 RESULTS

#### 3.1 Equilibrium Solution

The model achieved equilibrium after a spin up period of 4 model years, after which the volume average total kinetic energy  $1/V \int_V 0.5\rho(u^2+v^2) dV$  (Fig. 2a) reaches a plateau and then fluctuates around  $1.2 \text{ kg m}^{-1} \text{ s}^{-2}$  until the end of the simulation. Domain averaged temperature levels (Fig. 2b) show a strong seasonal signal, superposed to a declining trend from year 4 onward. Domain averaged salinity (Fig. 2c) shows a declining trend without clear seasonality.

The average surface velocity field from the ROMS (Fig. 3a) shows the characteristic surface circulation patterns in the region. North of  $36^\circ\text{N}$  the circulation is mainly south-eastward due to the

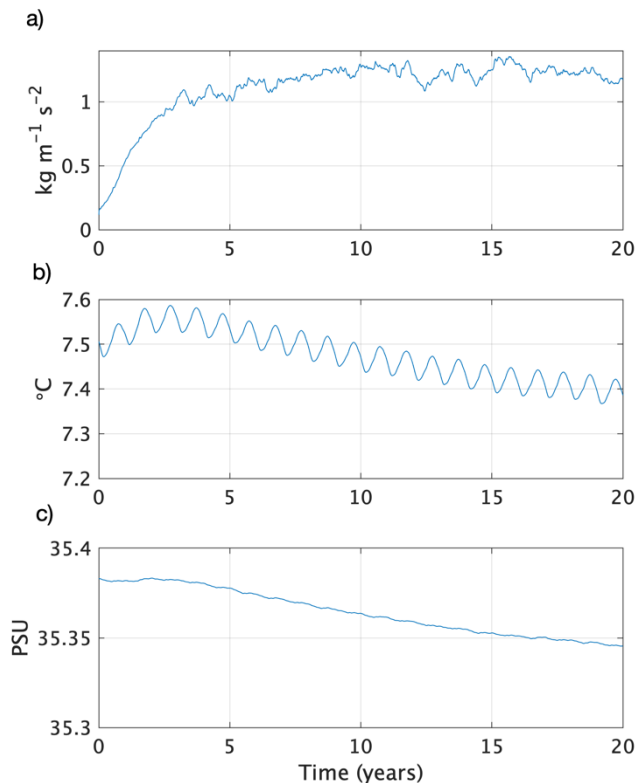


Figure 2. Time series of volume averaged a) kinetic energy; b) potential temperature; c) salinity.

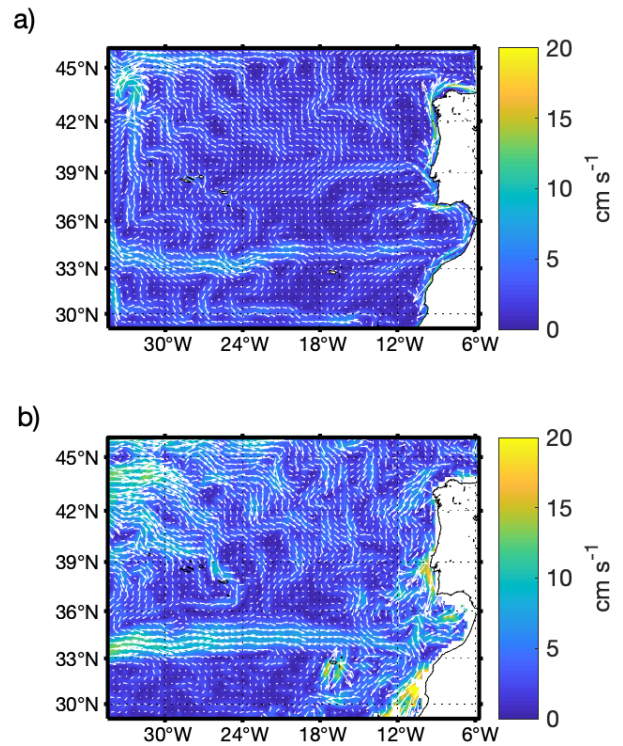


Figure 3. Average surface velocity from a) ROMS model and b) SVP climatology.

southward branches of the Gulf Current that separate approximately at  $54^\circ\text{W}$ , leaving the North Atlantic Drift and the southward PC between  $18^\circ$  and  $12^\circ\text{W}$  (Reverdin et al., 2003). East of the PC the circulation is influenced by the MO and the WIBUS. The main features of the average coastal circulation in the western Iberian shelf are the Cape São Vicente westward jet that flows along the slope of Gulf of Cadiz and the western Iberia coastal counter-flows. The poleward flow along the Iberian margin matches descriptions of the Portugal Coastal Counter-Current, that is known to bend anticyclonically when passing the north-western corner of the Iberian peninsula (Álvarez-Salgado et al., 2003), and of other coastal poleward counter-flows reported in the literature (Peliz et al., 2005, 2002).

Below  $36^\circ\text{N}$ , the AzC appears as the eastward jet between  $33^\circ$  and  $36^\circ\text{N}$ , clearly visible in Figure 3a until the Gulf of Cadiz, with maximum velocities of the order of  $10 \text{ cm s}^{-1}$ . The AzC partially turns south and joins the general westward and southward drift of the West Africa and the subtropical gyre. The eastward jet's location agrees with the well-known AzC location (Alves et al., 2002; Gould, 1985; Klein & Siedler, 1989), and it can be seen reaching the Gulf of Cadiz.

The comparison of the model average surface velocity field with the Surface Velocity Program climatology (Laurindo et al., 2017) (Fig. 3b) shows that the model velocities are generally lower than those of the SVP climatology. However, the position of the main features is well reproduced, especially the position of the AzC and the general south-eastward velocity field in the northern part of the



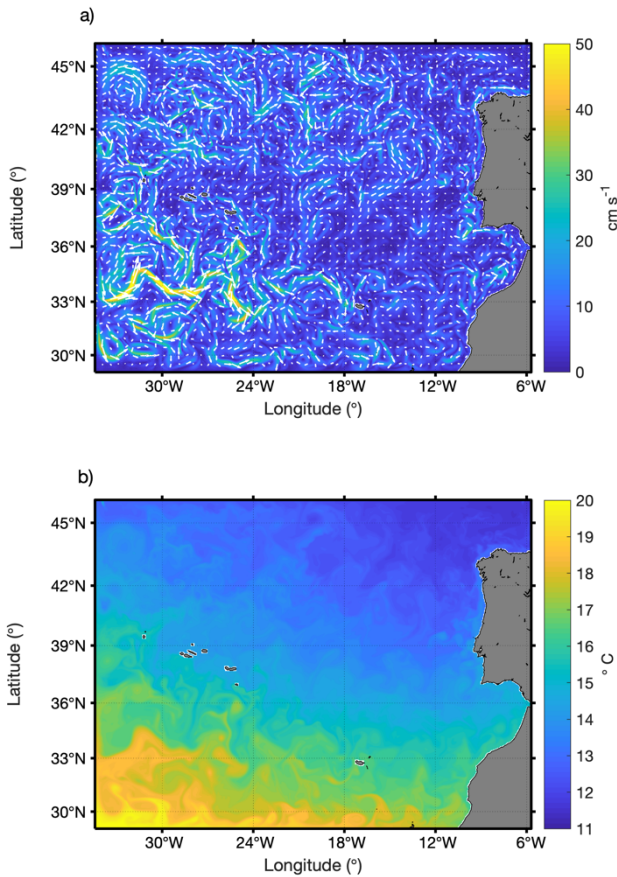


Figure 4. Instantaneous maps of a) surface velocity and b) sea surface temperature. Maps are for the 4<sup>th</sup> of March of S.Y. 18.

domain. The discrepancies highlight the limitations of the limited area modelling approach and the use of a climatological forcing. The first factor introduces errors at the boundaries e.g, the velocity imposed on the boundary is computed from geostrophy only while the SVP dataset is computed from real drifter velocities. The climatological forcing on the other hand limits the model response only to an annual cycle while the SVP dataset contains also interannual forcing effects.

### 3.2 The Azores Current

The average surface velocity field (Fig. 3a) shows the AzC as a purely zonal eastward jet. The instantaneous AzC, however, is known to have a large degree of meandering with mesoscale vortices shedding northward and southward of the mean current axis (Alves et al., 2002). However, the velocity field for 4 March of simulation year (S.Y.) 18 (Fig. 4a) shows the AzC as the predominant circulation feature in the region with instantaneous velocities up to 50 cm/s in the current axis. The axis itself is severely deformed, forming an cyclonic meander centred at approximately 32°W. South of the current axis three closed cyclonic circulations can be observed between the western boundary and 30°W. These cyclones have length scales on the order of 100 – 300 km and are present due to the pinching off of cyclonic vortices formed northward of the jet axis

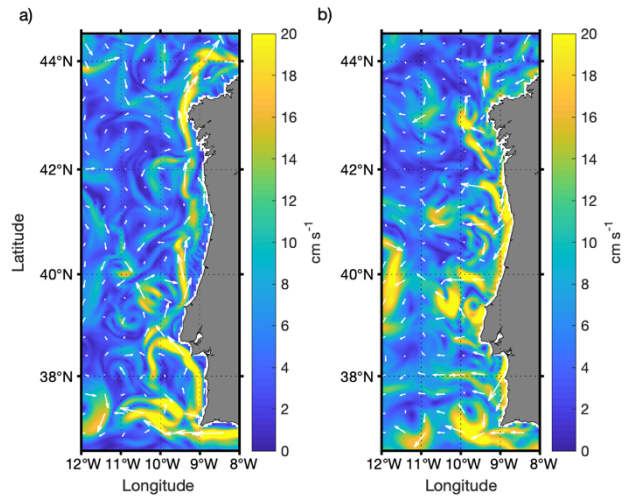


Figure 5. Instantaneous maps of model surface velocity for a) 13 January and b) 4 August of S.Y. 18.

(Alves et al., 2002). In a purely zonal jet, positive (cyclonic) vorticity is found northward of the jet axis and negative (anticyclonic) vorticity is found south of the jet axis. Although the idealization is far from being verified in this simulation, the situation depicted in Figure 4a conforms to this model. Indeed, just under the meander we can find a weak anticyclonic circulation.

The stirring (Abraham & Bowen, 2002) of the sea surface temperature (SST) field by the mesoscale circulation is visible in the SST map for 4 March S.Y. 18 (Fig. 4b), superposed on the gyre scale SST North-South gradient. The association of the AzC with the SST front is clearly observed as the position of the AzC meander coincides with the position of a strong change in SST. In addition, it is observed that the position of the large cyclone south of the current axis matches the position of a pool of cooler water, indication that the cyclonic had its origin north of the current axis and, as it moved south, carried with it the colder waters found north of the jet axis.

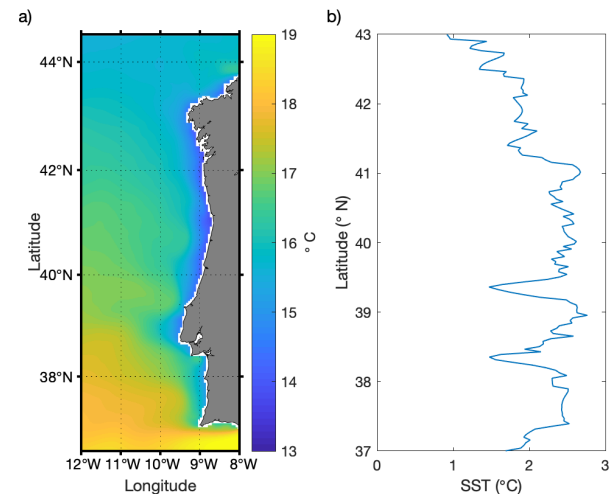


Figure 6. a) Average SST map; b) Upwelling index based on average coast (20 km) to offshore (500 km) SST differences. Positive values indicate colder waters at the coast.

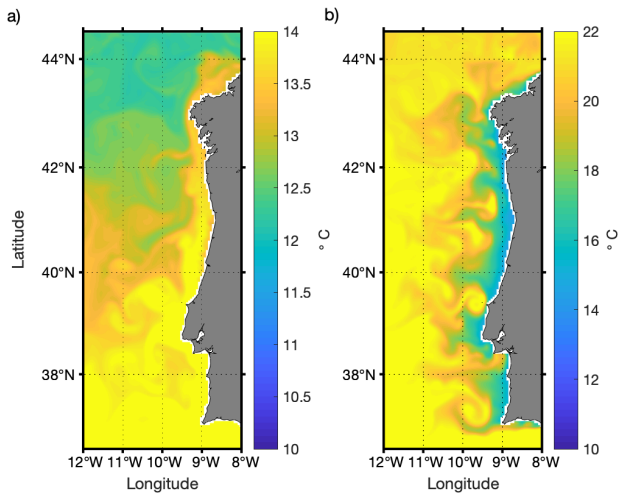


Figure 7. Instantaneous maps of model sea surface temperature for a) 13 January and b) 4 August of S.Y. 18.

### 3.3 The West Iberia Upwelling

The circulation in the WIBUS is highly seasonal and strongly influenced by mesoscale processes (Relvas et al., 2007). A winter surface velocity map for the 13 January of S.Y. 18 (Fig. 5a) shows some of the main elements of the winter circulation scheme proposed by Peliz et al. (2005). North of  $39^{\circ}$  N the coastal circulation is dominated by the poleward flow while the offshore flow is mainly southward. South of  $39^{\circ}$  N the influence of the Gulf of Cadiz circulation is clearly visible as an inflow to the southern Iberian basin (Fig. 5a). The summer situation is very different (Fig. 5b): the surface poleward flows are absent and the dominant coastal circulation is equatorward, forced by the summer equatorward winds. In addition, an offshore drift is clearly observable due to the generation of filaments and eddies by the upwelling front, that is known to be unstable to short wavelength instabilities (Durski & Allen, 2005).

The average SST field off the western Iberian coast (Fig. 6a) shows the signature of the West Iberia upwelling dynamics as a coastal strip of lower than average temperatures associated to successive upwelling cells along the coast. The SST difference between the coast and offshore waters (Fig. 6b) shows that this difference is about  $2.5^{\circ}\text{C}$  between  $37^{\circ}$  and  $41^{\circ}$  N and then decreases poleward, due to the decrease in offshore SST values (Fig. 6a).

Instantaneous SST maps for the same dates as Figure 5 show the difference in SST distributions for winter and summer. In winter (Fig. 7a) the western Iberian shelf is under the influence of the Gulf of Cadiz circulation whose inflow to the Iberian basin along the coast and subsequent entrainment in the Iberian Poleward Current brings warm water in to the Iberian shelf and slope (Peliz et al., 2005). In the summer (Fig. 7b) the upwelling is noticeable and the whole shelf shows SST colder than the offshore by

about  $6^{\circ}\text{C}$ . The mesoscale patterns in the SST distribution indicate the strong mesoscale dynamics of the upwelling front that presents several cold upwelling filaments extending 100 – 200 km offshore.

## 4 CONCLUSIONS

The Eastern basin of the North Atlantic between the subtropical and subpolar gyres presents a series of characteristics of oceanographic interest. The use of regional simulation models is a powerful tool to study the features that define the circulation in this region. High resolution climatological simulations allow simulating the equilibrium solution of the circulation and its intrinsic variability, providing necessary data to study the processes that control the circulation in the ECNA.

The AzC is a prominent feature of the circulation in the region. Its average position and its meandering character was unveiled by the simulation, showing that it controls the shape of the Azores Thermal Front and that thermal fluxes across the mean front position must be mediated by the mesoscale cyclones and anticyclones that are pinched off the AzC meanders.

The WIBUS is a seasonal upwelling system that in the winter is partially dominated by the Gulf of Cadiz circulation and the large scale offshore circulation. In the summer however, the coastal dynamics is strongly influenced by the upwelling front dynamics. The shelf and slope circulation is strongly modulated by mesoscale processes in both seasons.

To complement this type of studies, future work will use interannual forcing to study the response of the circulation to slow, large scale atmospheric processes such as the North Atlantic Oscillation, El Niño or the Atlantic Multidecadal Oscillation.

## 5 ACKNOWLEDGEMENTS

This study has been made in the project OBSERVA.FISH: Autonomous Observing Systems in Fishing Vessels for the Support of Marine Ecosystem Management, which has been funded under contract (PTDC/CTA-AMB/31141/2017) by the Portuguese Foundation for Science and Technology (Fundação para a Ciência e Tecnologia - FCT) and by EU FEDER POR-Lisboa2020 and POR-Algarve2020 programs. This work also contributes to the Strategic Research Plan of the Centre for Marine Technology and Ocean Engineering (CENTEC), which is financed by FCT under the contract UID/Multi/00134/2013 - LISBOA-01-0145-FEDER-007629.

## REFERENCES

- Abraham, E.R., Bowen, M.M., 2002. Chaotic Stirring by a Mesoscale Surface-Ocean Flow. *Chaos* 12: 373–381.
- Álvarez-Salgado, X.A., Figueiras, F.G., Pérez, F.F., Groom, S., Nogueira, E., Borges, A.V., Chou, L., Castro, C.G., Moncoiffé, G., Ríos, A.F., Miller, A.E.J., Frankignoulle, M., Savidge, G., Wollast, R., 2003. The Portugal coastal counter current off NW Spain: new insights on its biogeochemical variability. *Prog. Oceanogr.* 56: 281–321.
- Alves, M., Gaillard, F., Sparrow, M., Knoll, M., Giraud, S., 2002. Circulation patterns and transport of the Azores Front-Current system. *Deep Sea Res. Part II Top. Stud. Oceanogr., Canary Islands, Azores, Gibraltar Observations (Canigo) Volume II: Studies of the Azores and Gibraltar regions* 49: 3983–4002.
- Baringer, M.O., Price, J.F., 1997. Mixing and Spreading of the Mediterranean Outflow. *J. Phys. Oceanogr.* 27: 1654–1677.
- Chapman, D., 1985. Numerical Treatments of Cross-Shelf Open Boundaries in a Barotropic Coastal Ocean Model. *J. Phys. Ocean.* 15: 1060–1075.
- Durski, S.M., Allen, J.S., 2005. Finite-Amplitude Evolution of Instabilities Associated with the Coastal Upwelling Front. *J. Phys. Oceanogr.* 35: 1606–1628.
- Ellett, D.J., 1993. The north-east Atlantic: A fan-assisted storage heater? *Weather* 48: 118–126.
- Gould, W.J., 1985. Physical oceanography of the Azores front. *Prog. Oceanogr.* 14: 167–190.
- Haidvogel, D.B., Arango, H., Budgell, W.P., Cornuelle, B.D., Curchitser, E., Di Lorenzo, E., Fennel, K., Geyer, W.R., Hermann, A.J., Lanerolle, L., Levin, J., McWilliams, J.C., Miller, A.J., Moore, A.M., Powell, T.M., Shchepetkin, A.F., Sherwood, C.R., Signell, R.P., Warner, J.C., Wilkin, J., 2008. Ocean forecasting in terrain-following coordinates: Formulation and skill assessment of the Regional Ocean Modeling System. *J. Comput. Phys., Predicting weather, climate and extreme events* 227: 3595–3624.
- Haidvogel, D.B., Beckmann, A., 1999. Numerical Ocean Circulation Modeling, Series on Environmental Science and Management. IMPERIAL COLLEGE PRESS.
- Haynes, R., Barton, E.D., Pilling, I., 1993. Development, persistence, and variability of upwelling filaments off the Atlantic coast of the Iberian Peninsula. *J. Geophys. Res. Oceans* 98: 22681–22692.
- Jia, Y., 2000. Formation of an Azores Current Due to Mediterranean Overflow in a Modeling Study of the North Atlantic. *J. Phys. Oceanogr.* 30: 2342–2358.
- Johnson, J., Stevens, I., 2000. A fine resolution model of the eastern North Atlantic between the Azores, the Canary Islands and the Gibraltar Strait. *Deep Sea Res. Part Oceanogr. Res. Pap.* 47: 875–899.
- Klein, B., Siedler, G., 1989. On the origin of the Azores Current. *J. Geophys. Res. Oceans* 94: 6159–6168.
- Large, W.G., McWilliams, J.C., Doney, S.C., 1994. Oceanic Vertical Mixing: A Review and a Model with a Nonlocal Boundary Layer Parameterization. *Rev. Geophys.* 32: 363–403.
- Laurindo, L.C., Mariano, A.J., Lumpkin, R., 2017. An improved near-surface velocity climatology for the global ocean from drifter observations. *Deep Sea Res. Part I Oceanogr. Res. Pap.* 124, 73–92.
- Marchesiello, P., McWilliams, J.C., Shchepetkin, A., 2001. Open Boundary Conditions for Long-Term Integration of Regional Oceanic Models. *Ocean Model.* 3: 1–20.
- Peliz, A., Dubert, J., Marchesiello, P., Teles-Machado, A., 2007. Surface circulation in the Gulf of Cadiz: Model and mean flow structure. *J. Geophys. Res. Oceans* 112.
- Peliz, Á., Dubert, J., Santos, A.M.P., Oliveira, P.B., Le Cann, B., 2005. Winter upper ocean circulation in the Western Iberian Basin—Fronts, Eddies and Poleward Flows: an overview. *Deep Sea Res. Part I Oceanogr. Res. Pap.* 52: 621–646.
- Peliz, Á., Rosa, T.L., Santos, A.M.P., Pissarra, J.L., 2002. Fronts, jets, and counter-flows in the Western Iberian upwelling system. *J. Mar. Syst.* 35: 61–77.
- Pingree, R.D., Garcia-Soto, C., Sinha, B., 1999. Position and structure of the Subtropical/Azores Front region from combined Lagrangian and remote sensing (IR/altimeter/SeaWiFS) measurements. *J. Mar. Biol. Assoc. U. K.* 79: 769–792.
- Relvas, P., Barton, E.D., Dubert, J., Oliveira, P.B., Peliz, Á., da Silva, J.C.B., Santos, A.M.P., 2007. Physical oceanography of the western Iberia ecosystem: Latest views and challenges. *Prog. Oceanogr.* 74: 149–173.
- Reverdin, G., Niiler, P.P., Valdimarsson, H., 2003. North Atlantic Ocean surface currents. *J. Geophys. Res. Oceans* 108: 2-1-2–21.
- Shchepetkin, A.F., McWilliams, J.C., 2005. The regional oceanic modeling system (ROMS): a split-explicit, free-surface, topography-following-coordinate oceanic model. *Ocean Model.* 9: 347–404.
- Shchepetkin, A.F., McWilliams, J.C., 2003. A method for computing horizontal pressure-gradient force in an oceanic model with a nonaligned vertical coordinate. *J. Geophys. Res. Oceans* 108: 3090.
- Stramma, L., Müller, T.J., 1989. Some observations of the Azores Current and the North Equatorial Current. *J. Geophys. Res. Oceans* 94: 3181–3186.
- Tomczak, M., Godfrey, J.S., 2013. Regional Oceanography: An Introduction. Elsevier.
- Traon, P.-Y.L., Mey, P.D., 1994. The eddy field associated with the Azores Front east of the Mid-Atlantic Ridge as observed by the Geosat altimeter. *J. Geophys. Res. Oceans* 99: 9907–9923.
- Woodruff, S.D., Slutz, R.J., Jenne, R.L., Steurer, P.M., 1987. A Comprehensive Ocean-Atmosphere Data Set. *Bull. Am. Meteorol. Soc.* 68: 1239–1250.